BUTTERWORTH HEINEMANN

Polymer Vol. 36 No. 26, pp. 4943-4950, 1995

0032-3861/95/$10.00 + 0.00

Gas and water vapour transport in a polyketone terpolymer

M. A. Del Nobile* and G. Mensitieri
Department of Materials and Production Engineering, University of Naples 'Federico II', P. le Tecchio 80, 80125 Naples, Italy

and A. Sommazzi
Istituto Guido Donegani, via G. Fauser 4, 28100 Novara, Italy
(Received 30 September 1994; revised 13 February 1995)

Gas and water vapour transport properties of a polyketone terpolymer (0.93/0.07/1 ethylene/propylene/carbon monoxide) have been investigated and related to the polymer structure. Permeability tests have been performed at several temperatures (from 25 to about 65°C) with five different gases (oxygen, nitrogen, methane, ethane and carbon dioxide), evaluating permeabilities, diffusivities and solubilities. Their dependence on temperature was interpreted on the basis of apparent activation energies of permeation and diffusion (E_P and E_D) and of heats of solution (ΔH_S). The investigated polymer was found to be rubbery at the test temperatures (glass transition temperature is about 17°C), but the detected permeabilities are comparable to those of the glassy polymers widely used for packaging applications. Data obtained in this investigation on samples exposed to moulding temperatures (240°C) for 3 min were compared to gas permeation data (presented in a previous paper) obtained for samples exposed at that temperature for 33 min in order to assess possible effects on gas transport properties. Water vapour transport was analysed by performing both sorption (35, 34, 55 and 65°C) and permeation (35°C) experiments at several activities. The analysis of sorption isotherms revealed the occurrence of water clustering, which was confirmed by a reduction of water diffusivity as a function of water concentration in the polymer.

(Keywords: polyketone terpolymer; water vapour transport; gas permeability)

INTRODUCTION

Polyketones are attractive polymers for use in food packaging applications. This class of polymers is reported[1,2] to fulfil both processing and food preservation requirements. In fact they are one-step processable, have good impact properties, are dimensionally heat stable, are easily compoundable with other polymers used for food packaging (nylon, polycarbonate and ethylene–vinyl alcohol copolymer) and have good barrier properties competitive with those of nylon and poly(ethylene terephthalate) (PET)[3].

Olefins and carbon monoxide copolymerize with high conversions in the presence of group VIII transition-metal compounds[4,6]. The catalyst systems typically include a Pd(II) salt in methanol in combination with bidentate phosphine or bidentate nitrogen ligand, an acid and optionally an oxidant such as *p*-benzoquinone. The resulting copolymers, i.e. polyketones, are high-melting solids, showing a regular structure with alternating CO and olefin units. The ethylene/carbon monoxide copolymer has a melting temperature (T_m) of approximately 257°C. In order to process the material it must be heated to at least 25°C above the T_m. Since its thermal stability is too low to withstand such temperatures without decomposition, 5–10 mol% of a third monomer (e.g. propylene) can be introduced along the chain to overcome this deficiency. As the amount of propylene in the terpolymer increases, the T_m decreases and processing temperatures can be reduced below the decomposition temperature.

The polyketone investigated in the present study is a linear terpolymer consisting of alternating aliphatic and carbon monoxide groups, the aliphatic group being either polyethylene or polypropylene repeat unit, as shown below:

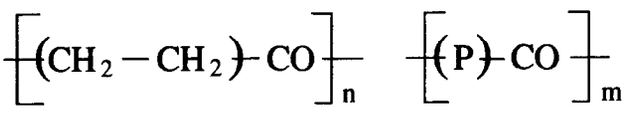

where 'P' is the propylene unit, and the ratio m/n is about 0.07. The $-CO-(C_2H_4)-$ units and the $-CO-(P)-$ units occur randomly throughout the polymer backbone.

This material is a semicrystalline rubbery polymer at 25°C. The barrier properties are reported to depend on the cooling protocol of the manufacturer[2], probably due to the different amount of crystallinity developed and to the different crystal shapes and dimensions.

Even though the thermal stability of this polymer at processing temperatures is greatly enhanced by the

* To whom correspondence should be addressed

presence of propylene units if compared to the ethylene/CO copolymer, there is still a degree of thermal instability due to thermolysis reaction occurring during prolonged exposure at processing temperatures. The decomposition mechanism is unknown and only limited information can be found in the literature[7,8]. Radicals formed during degradation are the main sources of branching, as also confirmed by a study carried out by means of *FT*i.r. spectroscopy on thermally treated samples[8].

The gas permeation process in rubbery polymers, like the investigated terpolymer, can be described in terms of a dissolution–diffusion mechanism. Henceforth, in the examination of gas transport properties, both the kinetic (diffusivity) and equilibrium (solubility) aspects need to be analysed.

The solubility process of low-molecular-weight compounds in semicrystalline rubbery polymers has been described[9–13] in terms of a 'reduced solubility'. In the case of semicrystalline rubbery polymers, it can be supposed that the amorphous fraction has characteristic thermodynamic properties which are independent of the level of crystallinity and that no molecules dissolve in the crystalline phase. This assumption is supported by experimental results reported for several polymer/low-molecular-weight compound systems[10,14,15]. On this basis we can express the solubility coefficient S of small molecules in semicrystalline polymers as a function of the amorphous volume fraction (α) and of the amorphous solubility coefficient (S^*) according to the following equation:

$$S = \alpha S^* \qquad (1)$$

S^* is generally dependent on penetrant concentration.

A fundamental thermodynamic theory of penetrant sorption in rubbery polymer matrices, which assumes the randomness of mixing, was originally introduced by Flory[16]. The water sorption phenomenon in rubbery polymers can be much more complex than reported above. In fact water sorption in moderately hydrophobic polymers, like the polyketone terpolymer under investigation, is frequently accompanied by water clustering as reported in the literature[17–20]. Zimm and Lundberg[21–24] theoretically modelled penetrant clustering, introducing 'cluster functions' which take into account the 'non-randomness' of penetrant–polymer mixing. The occurrence of penetrant clustering frequently manifests itself in a reduction of the diffusion coefficient, heat and entropy of dilution as the penetrant concentration increases[17–19].

In the present study gas permeation tests have been performed at different temperatures and pressures with several gases, differing in dimensions and polarizability, on semicrystalline terpolymer samples. The effect of melt processing time on gas transport properties was not found to be relevant. Water vapour sorption and permeation experiments were also performed. Sorption isotherms at 35, 45, 55 and 65°C were obtained. Permeation experiments were performed at 35°C at upstream pressures ranging from 4 to 25 Torr. The shape of the sorption isotherms as well as the results of permeation tests performed on the polymer suggest the occurrence of water clustering.

Finally, gas permeation as well as water sorption data of the terpolymer were compared with those obtained for 'cast' and bioriented commercial nylon-6 films, which are widely used in food packaging applications.

EXPERIMENTAL

Materials

The ethylene–propylene–CO terpolymer used in the present study was prepared with palladium catalyst, according to published procedures[4–6]. The resulting polymer (where the amount of the propylene–CO group is 7%, randomly distributed along the chain) is a white, highly crystalline solid with a limiting viscosity number (LVN) of 1.5 dl g^{-1}, measured in *m*-cresol at 100°C in a standard capillary viscosity measuring device. The glass transition temperature (T_g) is about 17°C and the melting point has been found to be around 220°C. Film samples of terpolymer were produced by compression moulding, heating the terpolymer up to a temperature 20°C above its melting point and cooling slowly. Since the polymer chemical structure changes due to exposure to the processing temperature, as mentioned above, two types of samples were compared. The first type, referred to in the following as 'type A' sample, was obtained by compression moulding the material at 240°C for 3 min; while the second type, referred to in the following as 'type B' sample, was obtained by compression moulding the material at 240°C for 33 min. In *Figure 1* is reported the apparent viscosity of melted polymer at 240°C as a function of moulding time at this temperature. A continuous increase of viscosity is evident. This effect should result from a certain degree of branching following exposure for a prolonged time to the processing temperature. In fact even though 'type A' and 'type B' samples show some differences in melt apparent viscosity, they are both soluble in *m*-cresol at 100°C, indicating that the amount of crosslinking, if present, is not relevant. The percentage crystallinity, estimated from X-ray diffraction, was about 42% for both kinds of samples.

For the sake of comparison, oxygen permeability measurements as well as water vapour sorption tests were also performed on commercial bioriented and 'cast' nylon-6 films (SNIA Tecnopolimeri, nylon-6 'cast', thickness = 0.02 mm and nylon-6 bioriented, thickness = 0.025 mm).

Gases were supplied by Matheson and the purities were the following: N_2 99.999%, O_2 99.95%, CO_2 99.998%, CH_4 99.995%, C_2H_6 99.99%. Gases were used without any further purification. Water used for sorption and permeation experiments was first distilled and then degassed by freezing–thawing cycles.

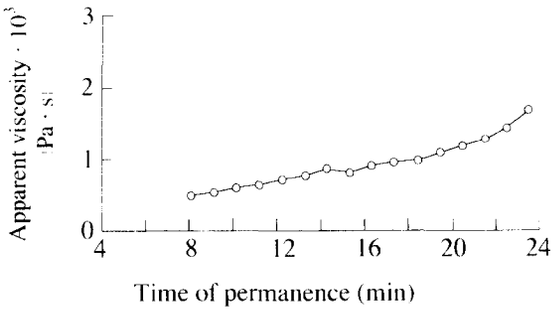

Figure 1 Melt apparent viscosity as function of holding time at 240°C

Methods

Apparent viscosity measurements of molten polymer were performed using a capillary rheometer (Rheograph model 2002 Goettfert).

Permeability tests with both gases and water vapour were performed using a technique based on the detection of the pressure increase at the downstream side of the polymer film pressurized at the upstream side. The polymer sheet was located in a gas-tight permeation cell separating the upstream and downstream chambers. Before the permeation test, each sample was allowed to desorb moisture eventually absorbed in the material during storage, degassing both the chambers for several days at about 10^{-4} Torr. Further details of the adopted experimental procedures are reported elsewhere[3].

The water vapour sorption apparatus consisted of a quartz spring placed in a water jacket glass cell with service lines to a solvent reservoir and to a pressure transducer. The pressure of water vapour was measured by means of a very sensitive capacitance transducer (MKS Baratron 221A, with an accuracy of 0.5% of the reading) whose range was chosen according to the operating pressures, while the vacuum level attained during desorption was checked by means of a Pirani or Penning manometer. The equilibrium sorption values as well as the sorption kinetics were determined at increasing solvent activities. The quartz spring used for these experiments had a sensitivity equal to 5 mg cm^{-1}. Spring elongation was monitored using a travelling microscope able to detect displacements as small as 0.005 mm.

Sample crystallinity was measured using a wide-angle X-ray diffractometer. Wide-angle X-ray diffractograms were obtained in transmission using a powder diffractometer (PW 1020 Philips). CuK_α radiation was used in the angular range 5–60°. The raw spectra were further analysed by Graphic Mathematical Package with a Unisys 1100 mainframe computer (Istituto Guido Donegani/Unisys).

Crystallinity was calculated by subtracting the amorphous halo from the original diffractogram between 5 and 40° and calculating the respective area values by digital integration.

RESULTS AND DISCUSSION

Gas transport

The solubility and diffusivity coefficients were evaluated by permeability tests. The diffusivity was calculated from the 'time lag' value according to the following equation[25]:

$$D = l^2/(6\theta) \quad (2)$$

where l is the sample thickness and θ is the measured time lag. The solubility coefficient has been determined as the ratio of detected permeability and diffusion coefficients, the latter being evaluated from equation (2), i.e.:

$$S = P/D \quad (3)$$

where P is the measured gas permeability.

Equations (2) and (3) presume the validity of Henry's law for gas sorption and of Fick's first law with constant diffusivity for gas transport, which are reasonable assumptions in the case of gas permeation in rubbery semicrystalline polymers[12].

Tables 1–5 report the diffusivity, solubility and permeability data obtained for N_2, O_2, CH_4, C_2H_6 and CO_2, at temperatures ranging from 25 to about 65°C. Permeability measurements were performed at upstream gas pressures equal to 0.1 MPa.

Table 1 Diffusivity, solubility and permeability data for nitrogen at several temperatures

Temperature (°C)	D (cm^2 s^{-1})	S (cm^3(STP)/cm^3 atm)	P (cm^3(STP)cm/cm^3 atm min)
25	2.28×10^{-9}	9.006×10^{-3}	1.23×10^{-9}
35	5.92×10^{-9}	7.78×10^{-3}	2.76×10^{-9}
45	1.53×10^{-8}	7.51×10^{-3}	6.92×10^{-9}
55	3.35×10^{-8}	7.72×10^{-3}	1.55×10^{-8}
61.5	5.52×10^{-8}	7.49×10^{-3}	2.48×10^{-8}

Table 2 Diffusivity, solubility and permeability data for oxygen at several temperatures

Temperature (°C)	D (cm^2 s^{-1})	S (cm^3(STP)/cm^3 atm)	P (cm^3(STP) cm/cm^3 atm min)
25	7.73×10^{-9}	1.386×10^{-2}	6.43×10^{-9}
35.5	1.603×10^{-8}	1.57×10^{-2}	1.15×10^{-8}
45	3.54×10^{-8}	1.457×10^{-2}	3.09×10^{-8}
55	6.74×10^{-8}	1.452×10^{-2}	5.88×10^{-8}
63	1.149×10^{-7}	1.326×10^{-2}	9.14×10^{-8}

Table 3 Diffusivity, solubility and permeability data for methane at several temperatures

Temperature (°C)	D (cm^2 s^{-1})	S (cm^3(STP)/cm^3 atm)	P (cm^3(STP) cm/cm^3 atm min)
25	8.73×10^{-10}	3.86×10^{-2}	2.022×10^{-9}
34.5	2.28×10^{-9}	3.68×10^{-2}	5.039×10^{-9}
45	7.05×10^{-9}	3.06×10^{-2}	1.292×10^{-8}
49.5	1.097×10^{-8}	2.90×10^{-2}	1.90×10^{-8}
54.2	1.631×10^{-8}	3.05×10^{-2}	2.989×10^{-8}

Table 4 Diffusivity, solubility and permeability data for ethane at several temperatures

Temperature (°C)	D (cm^2 s^{-1})	S (cm^3(STP)/cm^3 atm)	P (cm^3(STP) cm/cm^3 atm min)
25	1.191×10^{-10}	8.56×10^{-2}	6.11×10^{-10}
34.6	2.366×10^{-10}	1.43×10^{-1}	2.03×10^{-9}
45	7.325×10^{-10}	1.62×10^{-1}	7.11×10^{-9}
55	2.876×10^{-9}	1.09×10^{-1}	1.88×10^{-8}
61	5.28×10^{-9}	1.05×10^{-1}	3.34×10^{-8}

Table 5 Diffusivity, solubility and permeability data for carbon dioxide at several temperatures

Temperature (°C)	D (cm^2 s^{-1})	S (cm^3(STP)/cm^3 atm)	P (cm^3(STP) cm/cm^3 atm min)
25	1.49×10^{-9}	6.43×10^{-1}	5.75×10^{-8}
34.5	3.63×10^{-9}	5.54×10^{-1}	1.18×10^{-7}
39.5	6.45×10^{-9}	4.54×10^{-1}	1.76×10^{-7}
45	9.66×10^{-9}	4.29×10^{-1}	2.48×10^{-7}
49	1.37×10^{-8}	3.76×10^{-1}	3.09×10^{-7}
55	2.02×10^{-8}	3.69×10^{-1}	4.46×10^{-7}
60	3.10×10^{-8}	3.00×10^{-1}	5.59×10^{-7}

In the investigated temperature range these data are fairly well represented by a linear relationship relating the natural logarithm of the considered parameter to the reciprocal of absolute temperature. As a consequence the dependence on temperature of diffusion, solubility and permeability can be expressed as follows:

$$D = D_0 \exp\left(\frac{-E_D}{RT}\right) \quad (4)$$

$$S = S_0 \exp\left(\frac{-\Delta H_S}{RT}\right) \quad (5)$$

$$P = P_0 \exp\left(\frac{-E_P}{RT}\right) \quad (6)$$

where E_D is the apparent activation energy related to the diffusion process, ΔH_S is the heat of solution and E_P is the sum of E_D and ΔH_S. *Table 6* reports the evaluated values of E_D, D_0, ΔH_S and S_0. *Figure 2* reports measured values of E_D as a function of penetrant molecular diameter squared. A downward concavity is evident and it seems that no apparent diffusion activation energy is required for diffusion of penetrants that are sufficiently small. Interpretation and modelling of the dependence of apparent diffusion activation energy on penetrant molecular diameter is widely reviewed in the literature[26,27].

To assess the effect of structural change on gas transport properties, experimental gas permeation results obtained in this investigation on 'type A' samples were compared, in the case of oxygen and carbon dioxide, with those previously obtained[3] for 'type B' samples. Permeabilities at 25, 35 and 45 C for both polymers are reported in *Table 7* (data for 'type A' polymer were obtained at the reported temperatures by fitting experimental data by means of an Arrhenius expression). Permeabilities are only slightly lower in the case of 'type B' sample. Analogously, slight differences for the two samples were detected for diffusivities, solubilities, apparent activation energies and heats of solution.

These data suggest that prolonged exposure to high temperature does not substantially affect gas transport properties.

Water transport

Analysis of water transport in 'type A' terpolymer was performed by accomplishing both sorption and permeation tests.

Water sorption isotherms were determined at four different temperatures (35, 45, 55 and 65 C). Water activities were increased stepwise in order to evaluate diffusivities in a small range of penetrant concentrations. Cycles of three consecutive sorption tests were accomplished by increasing the activity by 0.1. Cycles were separated by desorption stages. In *Figures 3* and *4* is reported the percentage amount of water, referred to the weight of dry amorphous polymer, sorbed at equilibrium at the four investigated temperatures reported as a function of water pressure and activity. The mixing process was found to be slightly endothermic as will be discussed in the following section. In *Table 8* are reported the diffusivities measured at each temperature, averaged over the range of pressures adopted. The logarithm of diffusivity is fairly well fitted by a straight line if plotted as a function of the inverse of absolute temperature (*Figure 5*).

Permeation tests were performed only at 35 C and the measured permeabilities are reported as a function of the upstream pressure in *Figure 6*. As can be noted, water permeability markedly increases with pressure.

An example of a water vapour sorption isotherm is reported in *Figure 7* in terms of volume fraction of water (referred to the amorphous polymer fraction) sorbed at equilibrium in the polymer as a function of water vapour activity at 55 C. As shown in *Figure 7*, at all the investigated temperatures the curves obtained by fitting low-activity data points with the Flory–Huggins[16] equation cannot suitably fit sorption data in the entire activity range. The deviation of the high-activity data points from the reported curves seems to suggest non-randomness of the mixing between polymer and water molecules. In other words, it appears that water molecules once inside the polymer tend to aggregate with each other to form clusters at high activities.

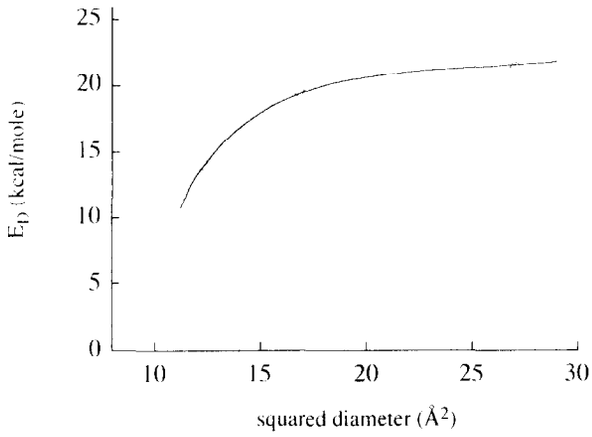

Figure 2 Apparent diffusion activation energy vs. squared penetrant diameter

Table 6 E_D, D_0, ΔH_S and S_0 for oxygen, nitrogen, carbon dioxide, ethane and methane for 'type A' sample

Gas	E_D (kcal mol^{-1})	D_0 (cm^2 s^{-1})	ΔH_S (kcal mol^{-1})	S_0 (cm^3(STP)/cm^3 atm)
Oxygen	14.07	152.6	−0.393	78.3×10^{-4}
Nitrogen	17.43	13766	0.947	18×10^{-4}
Carbon dioxide	17.25	6634	−4.47	3.56×10^{-4}
Methane	19.59	198800	−2.337	7.69×10^{-4}
Ethane	21.33	412500	0.573	2750×10^{-4}

Table 7 Permeability data of oxygen and carbon dioxide expressed in cm^3(STP) cm/cm^3 atm min for 'type A' and 'type B' samples

Gas	Temperature (C)	Type A	Type B
O_2	25	6.50×10^{-9}	5.08×10^{-9}
CO_2	25	5.75×10^{-8}	4.41×10^{-8}
O_2	35	1.11×10^{-8}	1.09×10^{-8}
CO_2	35	1.25×10^{-7}	9.58×10^{-8}
O_2	45	3.05×10^{-8}	2.4×10^{-8}
CO_2	45	2.46×10^{-7}	1.9×10^{-7}

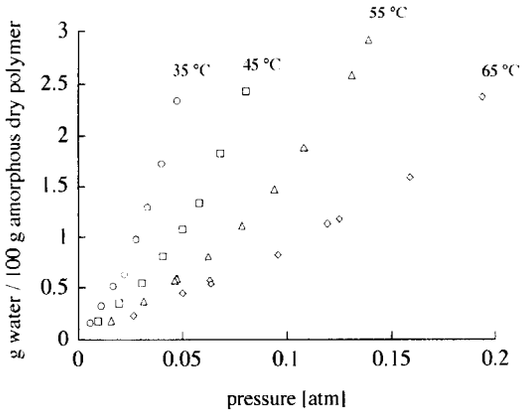

Figure 3 Amount of sorbed water vs. pressure of water vapour (after reference 29, reprinted by permission of John Wiley and Sons)

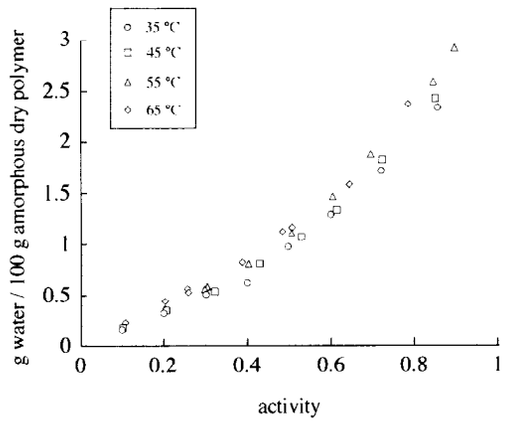

Figure 4 Amount of sorbed water vs. water vapour activity (after reference 29, reprinted by permission of John Wiley and Sons)

Table 8 Average water diffusivities evaluated at several temperatures from sorption experiments

Water average diffusivity ($cm^2 s^{-1}$)	Temperature (°C)
2.93×10^{-8}	35
5.65×10^{-8}	45
10.6×10^{-8}	55
17.1×10^{-8}	65

In fact the tendency of water molecules to cluster is relevant in moderately hydrophobic polymers and increases as the water concentration increases. Two 'cluster' functions have been introduced by Zimm and Lundberg[21–24] in their analysis of this phenomenon. The first, G_{AA}/V_A, is a measure of the tendency of sorbed molecules to form clusters. Values of G_{AA}/V_A greater than -1 indicate a disposition of penetrant molecules to form aggregates.

The second function, $1 + \phi_A G_{AA}/V_A$, represents a measure of cluster dimension and a value greater than 1 indicates the formation of penetrant aggregates. The term $\phi_A G_{AA}/V_A$ gives the average number of penetrant molecules surrounding a penetrant molecule in excess of the average penetrant concentration. G_{AA} represents the 'cluster integral', V_A is the partial molar volume

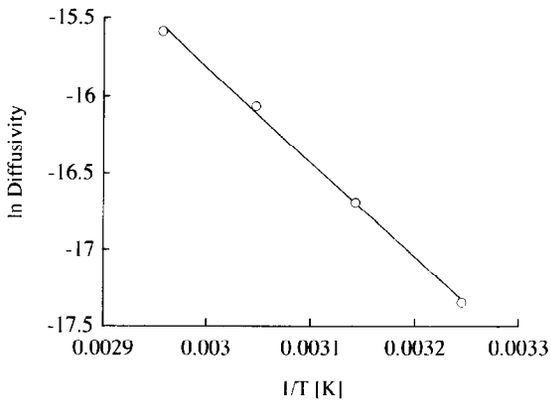

Figure 5 Arrhenius plot of water average diffusivity (after reference 29, reprinted by permission of John Wiley and Sons)

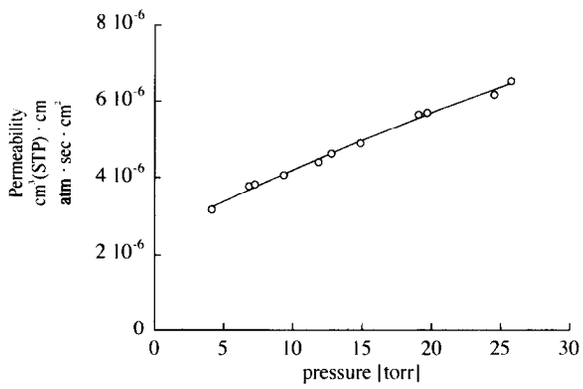

Figure 6 Water permeability coefficient vs. upstream pressure at 35°C (after reference 29, reprinted by permission of John Wiley and Sons)

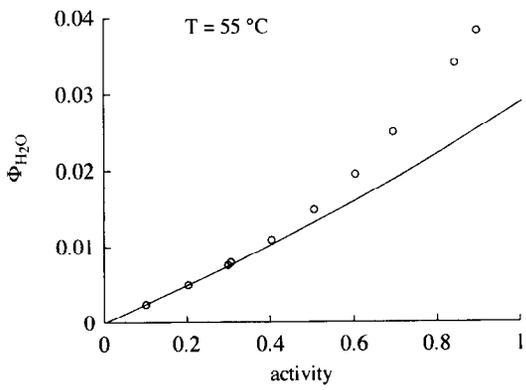

Figure 7 Volume fraction of sorbed water referred to the amorphous polymer fraction vs. water vapour activity at 55°C. The line represents the best fit of low-activity data points with the Flory–Huggins[16] equation (Flory–Huggins interaction parameter equal to 2.85)

of the penetrant and ϕ_A is the penetrant volume fraction.

In the following analysis it will be assumed that a_A is equal to p/p^0, where p is the pressure and p^0 is the water vapour pressure at the test temperature, and that polymer and penetrant volumes are additive, implying that partial molar volumes are equal to specific volumes.

The values of G_{AA}/V_A are higher than -1 for activities greater than 0.2 at all the investigated temperatures, as

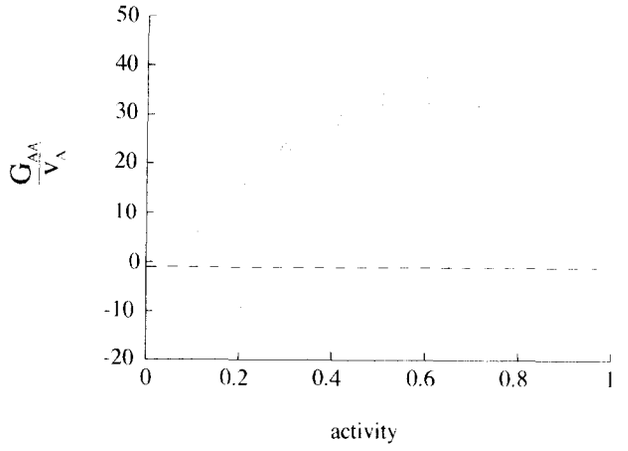

Figure 8 Value of G_{AA}/V_A reported as a function of water vapour activity at 35°C (□), 45°C (◇), 55°C (△) and 65°C (○) (after reference 29, reprinted by permission of John Wiley and Sons)

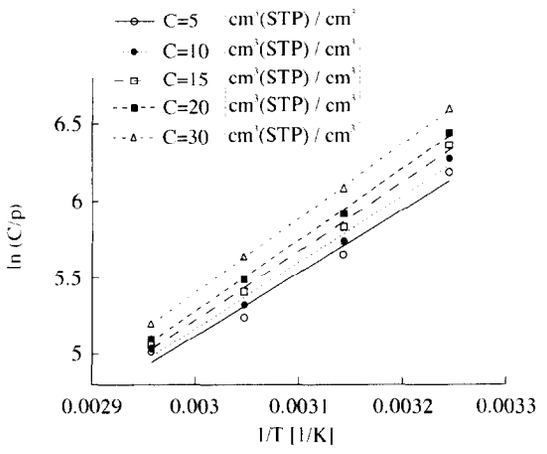

Figure 9 Van't Hoff plot of solubilities (ratio of water concentration and pressure of water vapour) evaluated at different levels of water concentration

Table 9 Values of G_{AA}/V_A for several water–polymer systems at water vapour activity equal to 0.7

Polymer	G_{AA}/V_A	Ref.
Polyisoprene (Cariflex IR 305) at 50°C	2150	19
Poly(dimethylsiloxane) at 40°C	660	17
Poly(dimethylmethylphenylsiloxane) at 40°C	840	17
Poly(3,3,3-trifluoropropylmethylsiloxane) at 40°C	760	17
Polyketone terpolymer at 45°C	30	this work
Ethyl cellulose at 25°C	14.4	20

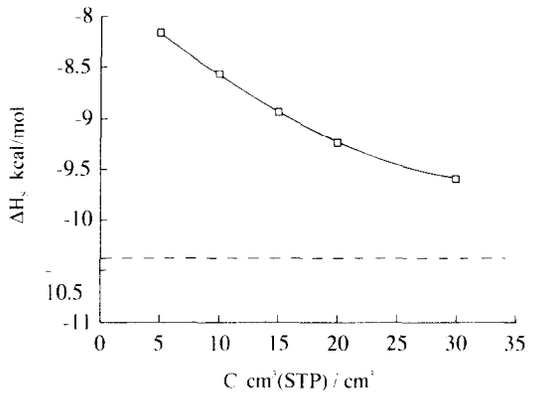

Figure 10 Heat of sorption reported as a function of water concentration. Dashed line represents water condensation enthalpy

shown in *Figure 8*, indicating a marked tendency of water molecules to cluster. Values of $1+\phi_A G_{AA}/V_A$ are greater than 1 at all the investigated temperatures and increase continuously with the activity, indicating that the average dimension of water clusters increases with water concentration. In *Table 9* are reported values of G_{AA}/V_A for polyketone terpolymer/water and for several other polymer/water systems at a water vapour activity equal to 0.7.

In *Figure 9* the logarithm of solubility (ratio of water concentration expressed as $cm^3(STP)/cm^3$(polymer) and water pressure expressed in atm) is reported as a function of $1/T$. Each curve represents the linear fitting of solubility data obtained at a fixed concentration level (5, 10, 15, 20 and 30 $cm^3(STP)/cm^3$(polymer)). Heats of sorption, evaluated from the slopes of these lines, decrease as the concentration increases, as reported in *Figure 10*. Mixing enthalpies were calculated from heats of sorption by adding the water condensation enthalpy (assumed to be equal to 10.39 kcal mol^{-1} (ref. 18)). The results of this analysis, reported in *Table 10*, show that the mixing process is endothermic and the related enthalpy decreases with concentration, as should be expected if clustering is occurring.

The formation of penetrant clusters should promote a decrease of diffusion coefficient due to the fact that a diffusion step involves the disaggregation of clusters. Owing to the small amount of sorbed water, errors affecting the evaluation of diffusivities obtained from differential sorption tests did not allow a reliable estimate of the variation that the diffusion coefficient eventually undertakes as penetrant concentration increases. For this reason an independent estimate of diffusivity was

Table 10 Values of heats of sorption ΔH_S and mixing enthalpy ΔH_M determined at several sorbed water concentration levels

Water concentration ($cm^3(STP)/cm^3$)	ΔH_S (kcal mol^{-1})	ΔH_M (kcal mol^{-1})
5	−8.16	2.23
10	−8.57	1.82
15	−8.93	1.46
20	−9.23	1.16
30	−9.59	0.78

obtained from permeation experiments[18]. In this work we present only preliminary results obtained at 35°C. In a permeation experiment:

$$\frac{d(Jl)}{dc_M} = \frac{d(P\Delta p)}{dc_M} = D(c_M) \qquad (7)$$

where J is the steady-state water flux, $D(c_M)$ is water diffusivity at concentration equal to c_M, Δp is the difference between upstream and downstream pressures, P is the water permeability, c_M is the water concentration in the polymer film at the upstream side, and l is the sample thickness. As a consequence the dependence of diffusion coefficient on the concentration ($D(c_M)$) can be obtained according to equation (7) from the plot reporting values of $P\Delta p$ as a function of concentration of water at the upstream side of polymer film (c_M). The

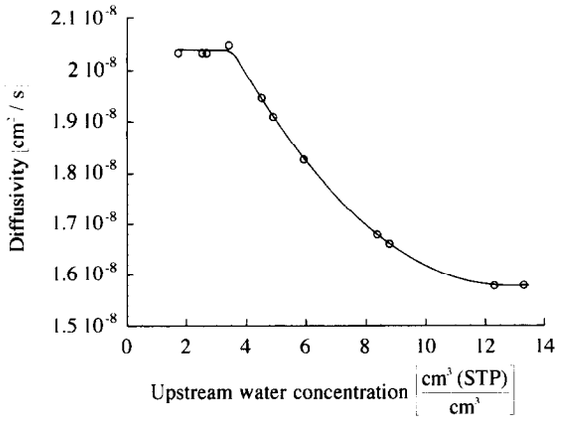

Figure 11 Water diffusivity evaluated from permeation experiments at 35°C reported as a function of sorbed water concentration at the upstream side of terpolymer film

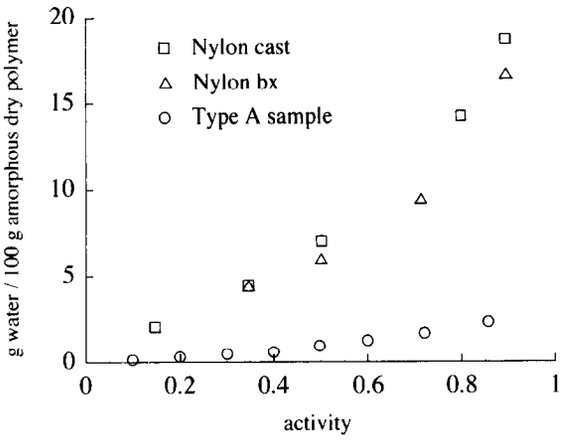

Figure 12 Water sorption isotherms at 35°C for 'type A' terpolymer sample and nylon-6 'cast' and bioriented films

obtained values of $D(c_M)$ as a function of c_M are represented in *Figure 11*. As expected, water diffusivities decrease as concentration increases above a certain value, confirming the occurrence of water clustering.

Comparison between terpolymer and nylon-6

In the following a comparison between the terpolymer under investigation and commercial nylon-6, widely used in food packaging applications, is briefly presented. The analysis is limited to oxygen permeation at 25°C and water sorption at 35°C.

Water sorption isotherms were determined for both 'cast' and bioriented nylon-6 at 35°C; the results are compared with those of 'type A' terpolymer in *Figure 12*. As expected, the amount of sorbed water is much higher in the case of nylon-6 due to the high interaction of water with amidic moieties. The breakage of hydrogen bonds brought about by sorbed water in nylon-6 causes a considerable plasticization of the system. In fact T_g values for both types of nylon-6 at different levels of sorbed water concentration theoretically evaluated by means of the equation proposed by Moy and Karasz[28] are strongly reduced by water. In *Table 11* are reported the evaluated T_g values in the case of bioriented nylon-6/water system.

Water diffusion coefficients determined from integral

Table 11 Calculated T_g values for bioriented nylon-6/water and polyketone terpolymer/water systems at 35°C for different amounts of sorbed water

	Sorbed water (g water/ 100 g amorphous phase)		Calculated T_g (°C)	
Water activity	Nylon	Terpolymer	Nylon	Terpolymer
0	0	0	46.5	17
0.347	4.40	0.569	14.3	4.8
0.502	6.00	0.968	6.2	−2.7
0.714	9.50	1.706	−13.4	−14.7
0.897	16.60	2.522	−34.6	−25.7

Table 12 Oxygen permeability data at 25°C for 'type A' terpolymer and 'cast' and bioriented nylon-6

Materials	O_2 permeability (cm^3(STP) cm/cm^3 atm min)
Type A terpolymer	6.50×10^{-9}
Nylon-6 cast	8.50×10^{-9}
Nylon-6 bioriented	5.20×10^{-9}

sorption tests in the case of nylon-6 are about one order of magnitude lower than in the case of terpolymer, and are strongly dependent on water concentration.

In *Table 12* are reported oxygen permeability values for 'type A' terpolymer as well as bioriented and 'cast' nylon-6. Permeability values for terpolymer are lower than in the case of 'cast' nylon-6, while they are very close to that determined in the case of bioriented film. It is worth noting that, while the terpolymer is rubbery at 25°C, both nylons are glassy ($T_g \cong 45$°C).

Owing to strong plasticization caused by sorbed water, oxygen permeability in nylon-6 films is expected to increase in high-humidity conditions much more than in the case of the examined terpolymer. In fact, the T_g depressions of the terpolymer/water system, as evaluated by means of the equation proposed by Moy and Karasz[28], are lower in the case of the terpolymer as reported in *Table 11*.

CONCLUSION

Gas permeation measurements performed on an ethylene/propylene/carbon monoxide (0.93/0.07/1) polyketone terpolymer with different gases have shown good barrier properties notwithstanding the fact that the test temperatures were above the polymer glass transition temperature. The good barrier properties of this polymer are competitive with those of nylon-6, poly(ethylene terephthalate) (PET) and polycarbonates.

In the range of investigated temperatures, permeability, diffusivity and solubility data were successfully correlated by Arrhenius and van't Hoff type relationships.

Changes in the backbone structure due to prolonged exposure to temperatures used for polymer processing do not substantially change gas transport properties of the polyketone terpolymer.

The shape of water sorption isotherms suggests the occurrence of water molecules clustering in the polymer matrix. This evidence was confirmed by the

decrease of water polymer mixing enthalpy with water concentration.

Consistent with significant association of water molecules, the water diffusion coefficient measured from permeation experiments was found to decrease with the amount of sorbed molecules.

Compared to the case of nylon-6, the lower plasticization of terpolymer in the presence of water guarantees a higher stability of gas barrier and mechanical properties under conditions of high relative humidity.

REFERENCES

1 Korcz, W. H., Kastelic, J. R., Dangayach, K. C. and Armer, T. A. Eur. Pat. Appl. 0306115 A2, September 1988
2 Gerlowski, L. E. and Kastelic, J. R. US Pat. 5077385, December 1991
3 Del Nobile, M. A. Mensitieri, G., Nicolais, L., Sommazzi, A. and Garbassi, F. *J. Appl. Polym. Sci.* 1993, **50**, 1261
4 Drent, E. Eur. Pat. Appl. 121965, 1984
5 Drent, E. Eur. Pat. Appl. 181014, 1986
6 van Broekhoven, J. A. M., Drent, E and Klei, E. Eur. Pat. Appl. 213671, 1987
7 Chien, J. C. W. and Zhao, A. X. *Polym. Degrad. Stab.* 1993, **40**, 257
8 Conti, G. and Sommazzi, A. *J. Mol. Struct.* 1993, **294**, 275
9 Michaels, A. S. and Parker, R. B. Jr *J. Polym. Sci.* 1959, **41**, 53
10 Michaels, A. S. and Bixler, H. J. *J. Polym. Sci.* 1961, **50**, 393
11 Michaels, A. S. and Bixler, H. J. *J. Polym. Sci.* 1961, **50**, 413
12 Koros, W. J. and Hellums, M. W. in 'Encyclopedia of Polymer Science and Engineering', Suppl. Vol. (Eds H. F. Mark, N. M. Bikales, C. G. Overberger, G. Menges and J. I. Kroschwitz), Wiley, New York, 1990
13 Klute, C. H. *J. Appl. Polym. Sci.* 1959, **1** (3), 340
14 Bixler, H. J. and Sweeting, O. J. in 'The Science and Technology of Polymer Films', Vol. 2 (Ed. O. J. Sweeting), Wiley, New York, 1971
15 Weinkauf, D. H. and Paul, D. R. in 'Barrier Polymers and Structures' (Ed. W. J. Koros), ACS Symp. Ser. 423, American Chemical Society, Washington, DC, 1990, Ch. 3
16 Flory, P. J. 'Principles of Polymer Chemistry', Cornell University Press, Ithaca, NY, 1953
17 Barrie, J. A. and Machin, D. *J. Macromol. Sci. (B)* 1969, **3**, 645
18 Barrie, J. A. and Machin, D. *Trans. Faraday Soc.* 1971, **67**, 244
19 Barrie, J. A., Machin, D. and Nunn, A. *Polymer* 1975, **16**, 811
20 Yasuda, H. and Stannett, V. *J. Polym. Sci.* 1962, **57**, 907
21 Zimm, B. H. *J. Chem. Phys.* 1953, **21**, 934
22 Zimm, B. H. and Lundberg, J. L. *J. Phys. Chem.* 1956, **60**, 425
23 Lundberg, J. L. *J. Macromol. Sci. (B)* 1969, **3**, 693
24 Lundberg, J. L. *J. Pure Appl. Chem.* 1972, **31**, 261
25 Crank, J. 'The Mathematics of Diffusion', 2nd Edn, Clarendon, Oxford, 1975
26 Kumins, C. A. and Kwei, T. K. in 'Diffusion in Polymers' (Eds J. Crank and G. S. Park), Academic Press, London, 1968, Ch. 4
27 Stern, S. A. and Trohalaki, S. in 'Barrier Polymers and Structures' (Ed. W. J. Koros), ACS Symp. Ser. 423, American Chemical Society, Washington, DC, 1990, Ch. 2
28 Moy, P. and Karasz, F. E. in 'Water in Polymers' (Ed. S. P. Rowland), ACS Symp. Ser. 127, American Chemical Society, Washington, DC, 1980
29 Mensitieri, G., Del Nobile, M. A., Sommazzi, A. and Nicolais, L. *J. Polym. Sci., Polym. Phys. Edn* 1995, **33** in press